CHAPTER 8

TEST RESULTS, THEIR INTERPRETATION, AND CONCLUSION

8.1 The S-beam Model

The formation of the incipient crack at the support, the development of the first crack at the centre-span, and the termination of the test refer respectively to the following values of dead-plus-live load factor: 1.387, 1.526, and 2.769. The last, although not corresponding to complete collapse, is unquestionably high in comparison with the expected 1.520 on the 1.4D + 1.7L basis. The milestone connotes that the ACI's approach for proportioning reinforced concrete member under the combined influence of bending, torsion, and shear brings ample safety in particular regard to the collapse load level.

Figure 8.1 presents graphically the relationship between the load and the centre-span deflection. The broken line is analytical, emanating from application of relation (5.17). At the service load D + L the recorded centre-span deflection amounts to 0.272 centimetre, the deflection-to-length ratio being 1:1,113. The computation for the analytical load-deflection relation draws on the value of the moment of inertia I referring to the gross section of the beam and on an average elastic modulus of 0.2118×10^6 kilogrammes per square centimetre. The calculation of this value of Young's modulus admits validity of ACI's empirical relation dependent on the density and 28 days' strength of the representative cylinder. At the service load level the actual deflection measures 1.67 times the theoretical magnitude.

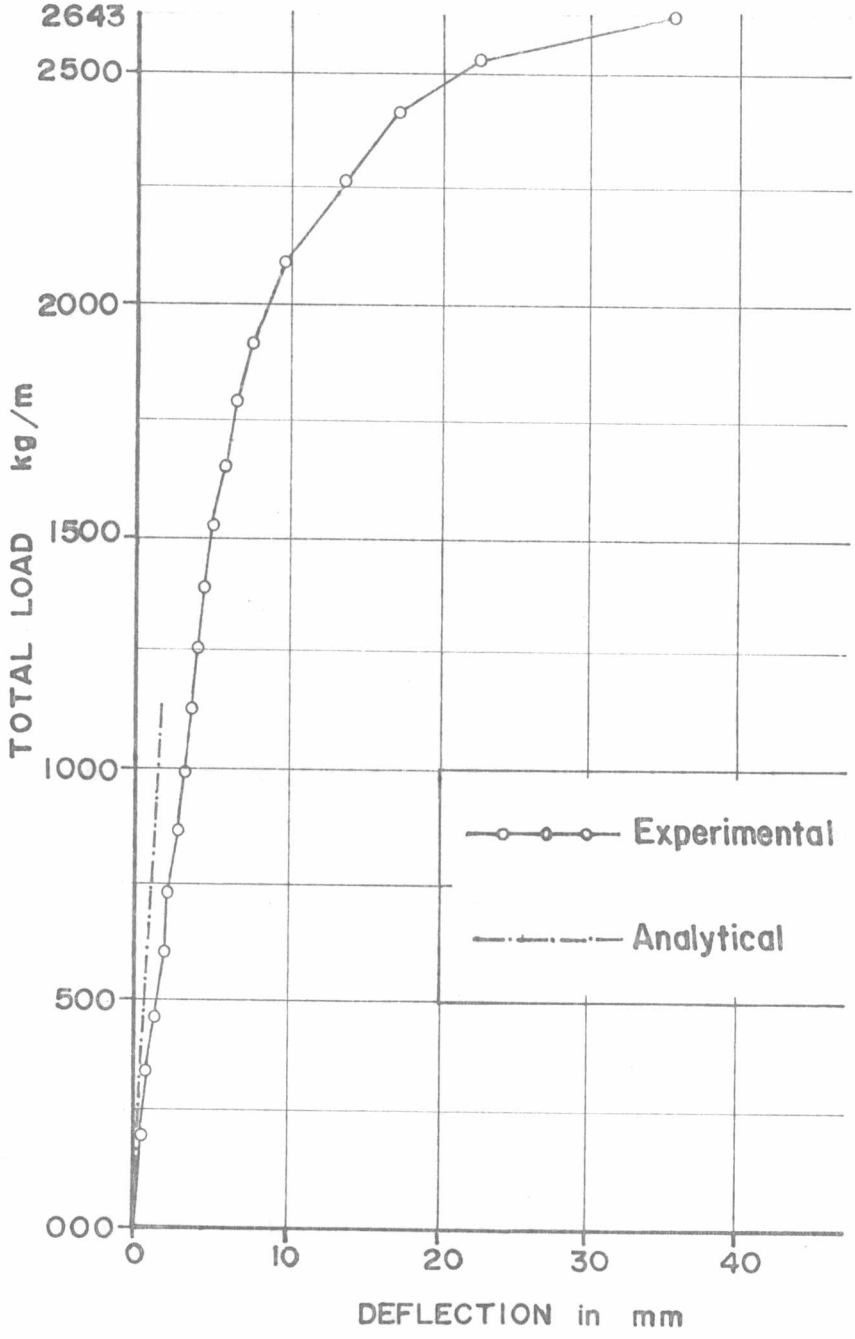

FIGURE 8.1 S-beam Model; Relation between Load and Center-span Deflection

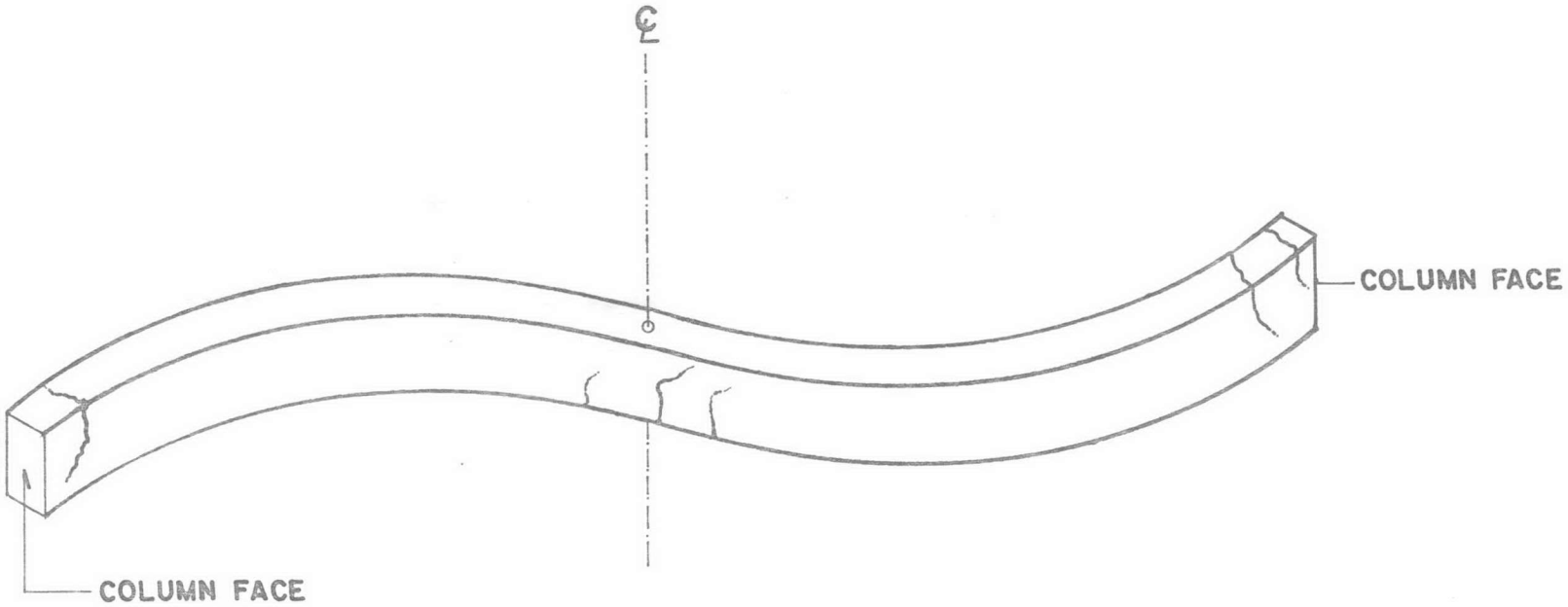

FIGURE 8.2 Sketch of Interesting Cracks on S-beam Model

The sketch of Figure 8.2 recasts the modes of vital cracks on the model. The appearance of the extended incipient crack on the intrados at a location bordering on the support, without a contemporary trace on the extrados, conveys cross-sectional asymmetry in respect of strength. This trait is not at all peculiar in view of: (i) difference in curvilinear length between the intrados and the extrados in reference to the distance from the centre-span to the support; and (ii) contradictory influences of torsion and shear on the extrados. One can assimilate justification for the first argument upon examining Figure 8.3(a). The intrados, being longitudinally shorter than the extrados, can obviously suffer a smaller extent of twist. Corresponding to an identical angle of twist the intrados, of all the vertical laminae, tends to undergo the severest state of stress. Figures 8.3(b) and 8.3(c) stand in support of the second argument. The exemplified element on the intrados experiences torsional and shearing influences of like sense. Contrariwise the element on the extrados identifies with torsional and shearing influences of contradictory sense, and hence yields predominantly to the bending effect. Without question as far as the marginal region is concerned the intrados remains the weakest under combined action of torsion and shear.

It again follows that the marginal portion of the uppermost longitudinal bar appropriate to the intrados withstands critical tension, hence meriting scrutiny. A distance of 9 centimetres separates the centre of the gauge glued to the focussed bar from the support, comparing insignificantly with the length 1.513 metres of the half-beam. The mounted gauge's position is therefore considered referable to the very

end of the beam, the theoretical location of critical flexural state. With an average elastic modulus of 2.03×10^6 kilogrammes per square centimetre of the steel the strain-to-stress conversion generates the load-stress curves given in Figure 8.4. A tensile stress of 4,260 kilogrammes per square centimetre corresponds to the termination of the test (load factor = 2.769). Observing an average maximum strength of 5,027 kilogrammes per square centimetre of the steel (Appendix D) it can be postulated that the actual dead-plus-live load factor pertinent to the collapse of the model lies in the neighbourhood of 3.267.

The tensile stresses in the bottom longitudinal bars at centre-span average: 1,625 kilogrammes per square centimetre at service load level; and 3,850 kilogrammes per square centimetre at termination of test. Conversion of strains detected from rosette-impersonating gauges at centre-span into stresses leads to the following magnitudes of concrete principal stress: 138 kilogrammes per square centimetre at service load level; and 215 kilogrammes per square centimetre at early development of the first centre-span crack.

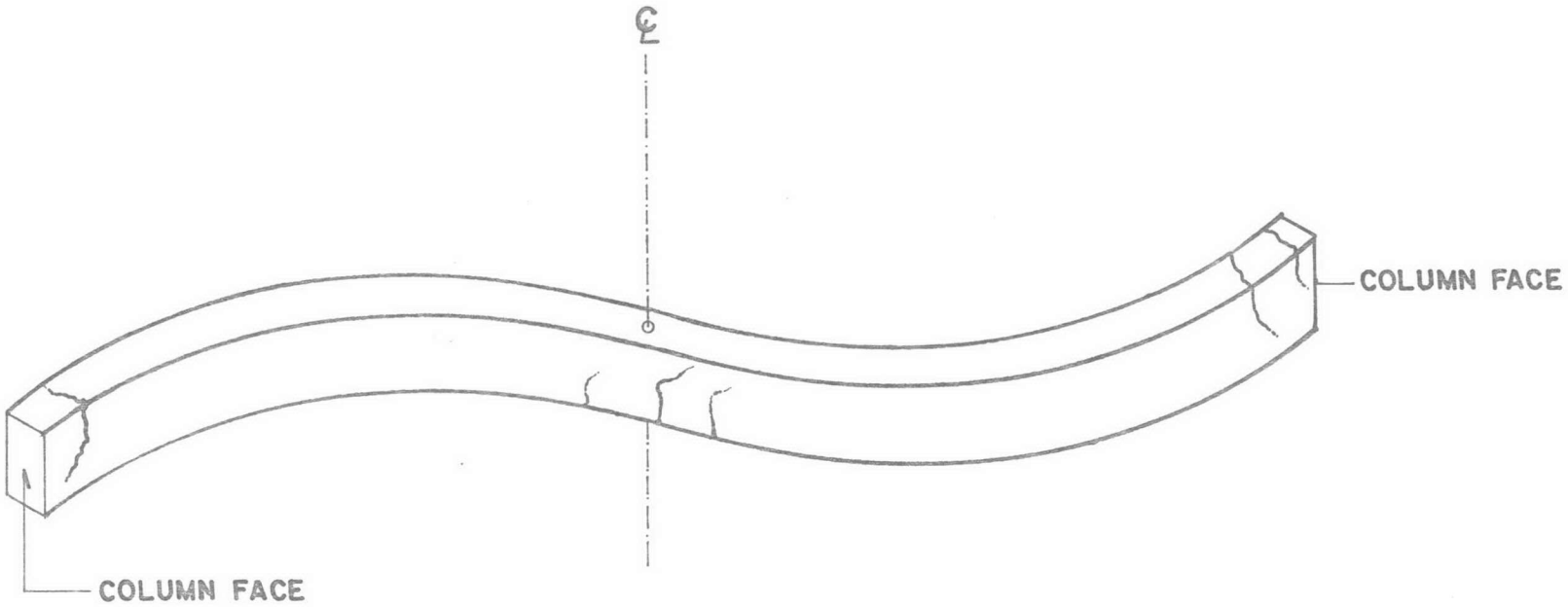

FIGURE 8.2 Sketch of Interesting Cracks on S-beam Model

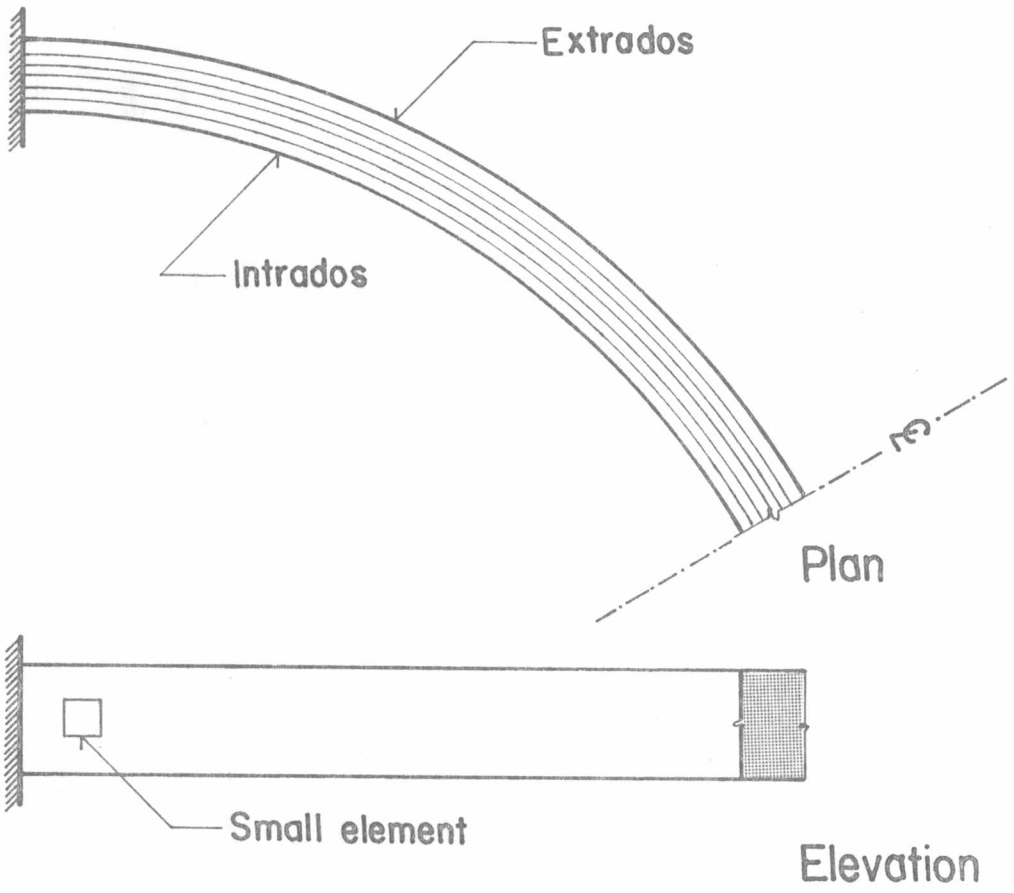

(a) Difference in length of vertical laminae

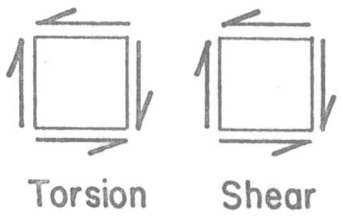

(b) Element on intrados

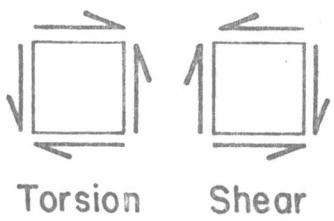

(c) Element on extrados

FIGURE 8.3 Diagram Aiding Inference of Cracking Asymmetry at Support

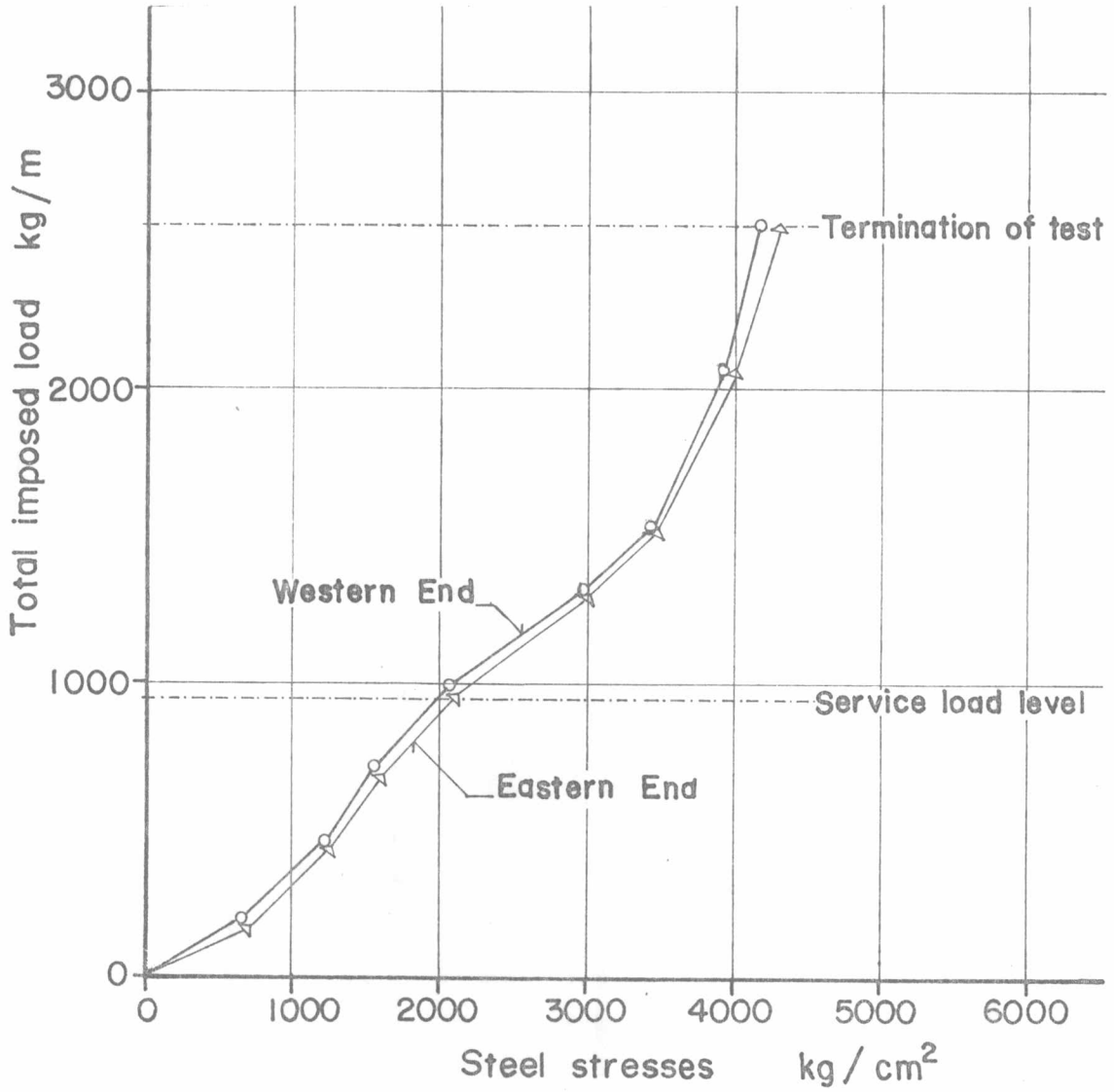

FIGURE 8.4 S-beam Model; Relation between Load and Critical Stress in Critical Longitudinal Reinforcement

8.2 The Z-beam Model

An extensive discussion apropos of the Z-beam model is omitted since its behaviour assimilates parallelism to the S-beam model's. Near each support the inner vertical face of the beam, likened to the S-beam's intrados, identifies with the vital diagonal crack resulting from combined influence of critical torsion and shear. Figure 8.5 gives a sketch of consequential crack paths. The following dead-plus-live load factors are inherent: 1.351 at the formation of the incipient crack at the support; 1.470 at the development of the first crack at the centre-span; 2.256 at the termination of the test; and 2.631 at the postulated collapse load level. The predicted aggregated ultimate load factor on the 1.4D + 1.7L basis registers 1.520. The curves of Figure 8.6 record variation of critical tensile stresses in longitudinal bars proportioned to resist negative bending plying with torsion at the supports. Figure 8.7 furnishes a comparison between the actual and analytical load-deflection curves, the deflection belonging to the centre-span.

8.3 Concluding Remarks

The following values of the aggregated load factor relevant to the S-beam model are arrayed: 1.387 at formation of incipient crack near support; 1.520 at expected code-wise ultimate load level; and 3.267 at probable actual collapse load level. Of consequence the level to which the ACI's 'ultimate load' refers heretofore remains ambiguous. It should

be said that the ACI's rules for proportioning members subject to combined bending, torsion, and shear are immensely satisfactory in respect of collapse, but somewhat otherwise of first crack formation. At any rate the load belonging to the very first crack on the S-beam model amounts to as high as 90.0 per cent of the code-wise ultimate value, a parallel extent of 89.9 per cent being appropriate to the Z-beam model. An average 10.1 per cent departure of the first crack load from the code-wise ultimate milestone is envisaged. The disparity is judged as insignificant seeing that in actuality such building components as floor beams are rearely given to overloading. Rather they normally carry imposed (live) loads of much lower intensities than the conventionally designated ones. The ACI's doctrine is therefore viewed as totally admissible insofar as buildings are concerned.

Nevertheless a strictly conservative designer may still be discontented with the immaterial degree of imperfection. Should he desire an ideally accurate agreement between the first crack level and the code-wise ultimate value he is advised to adjust the ACI's 1.4D + 1.7L to 1.54D + 1.87L.

One may elect to revert to the criteria set forth in the Australian Code, the well-known rules in universal use from time immemorial to 1970, the lapse marking unavailability of highly dependable principles governing the design of reinforced concrete members submitted to simultaneous influence of bending, torsion, and shear. Instrumentalisation of the Australian Code will always culminate in adoption of larger cross-sectional dimensions in comparison to application of the ACI Code at issue.

Emphasis should be placed on the misleading form of an expression contained in the 1977 ACI Code, as brought to notice in Appendix C. Acceptation of validity of the erroneous relation may spell discredit upon the user.

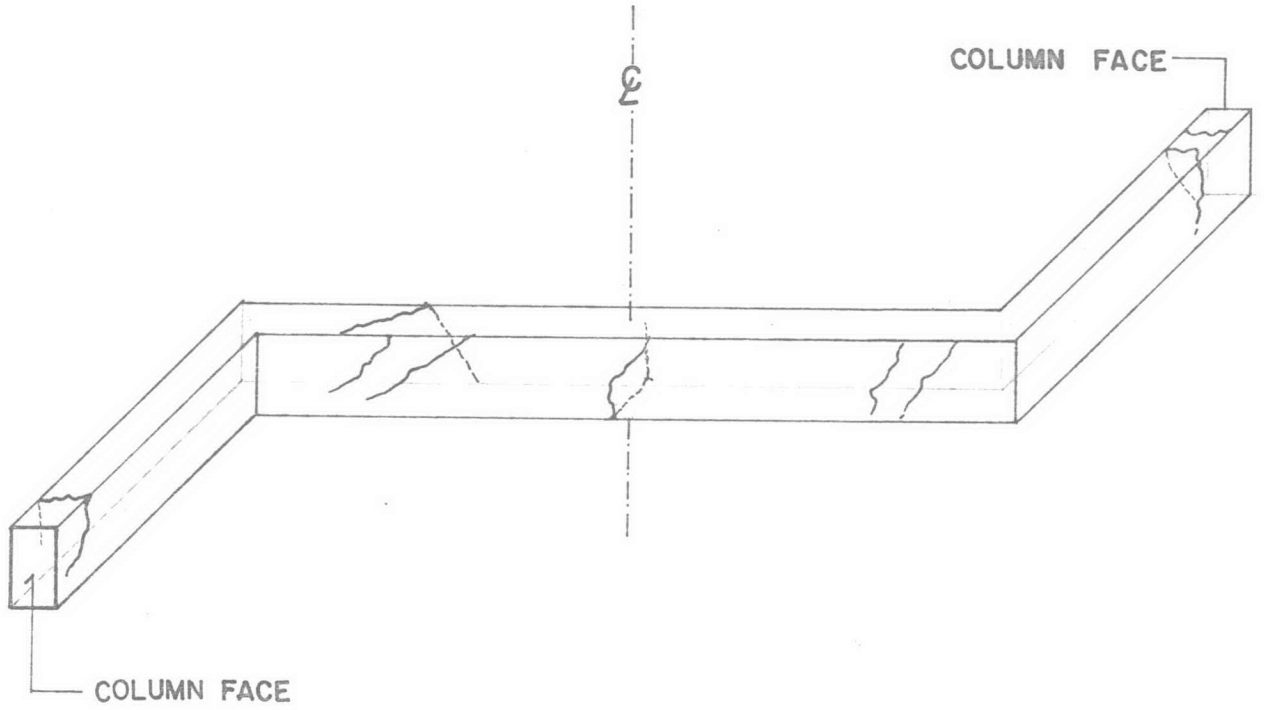

FIGURE 8.5 Sketch of Interesting Cracks on Z-beam Model

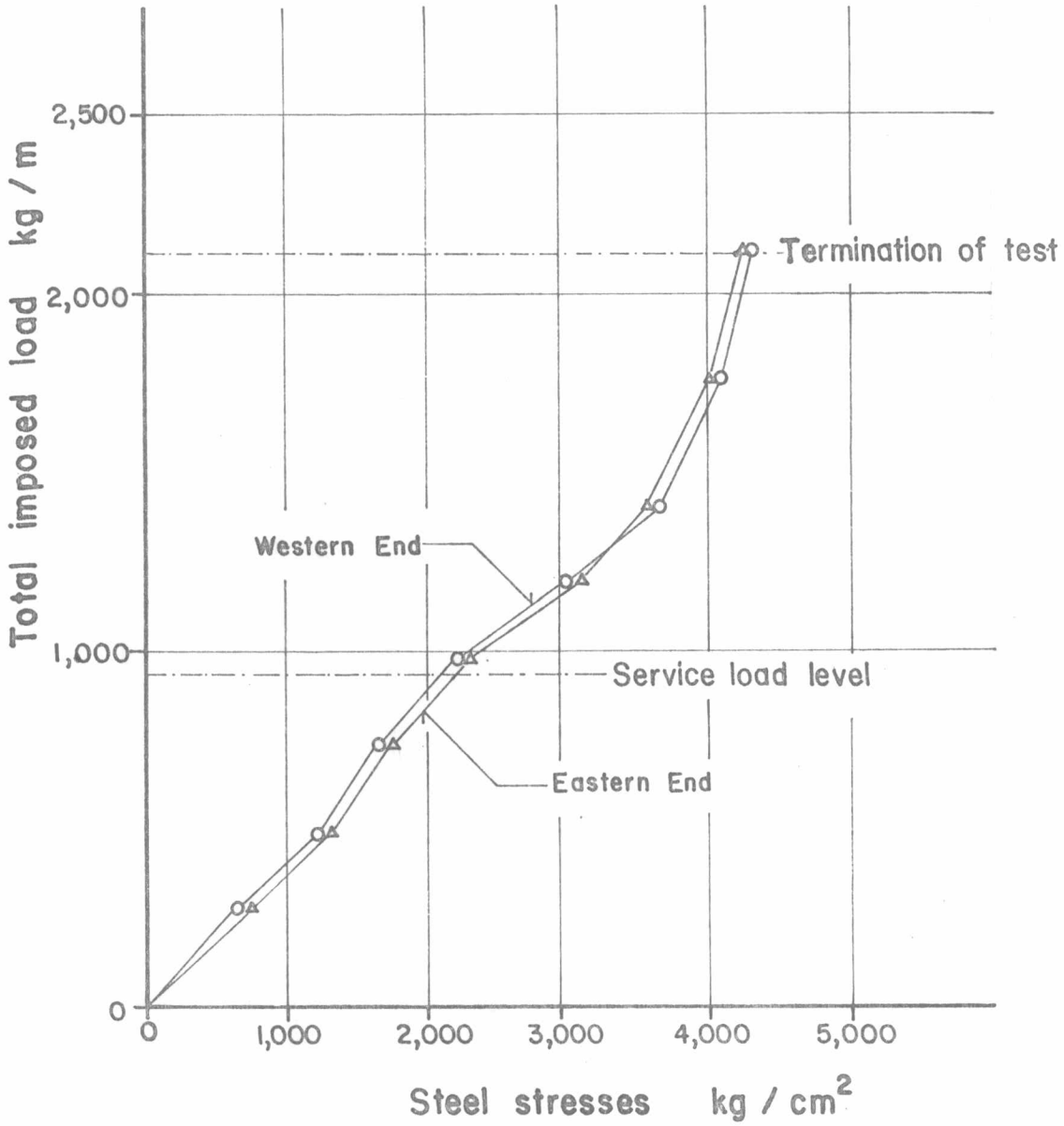

FIGURE 8.6 Z – beam Model; Relation between Load and Critical Stress in Critical Longitudinal Reinforcement

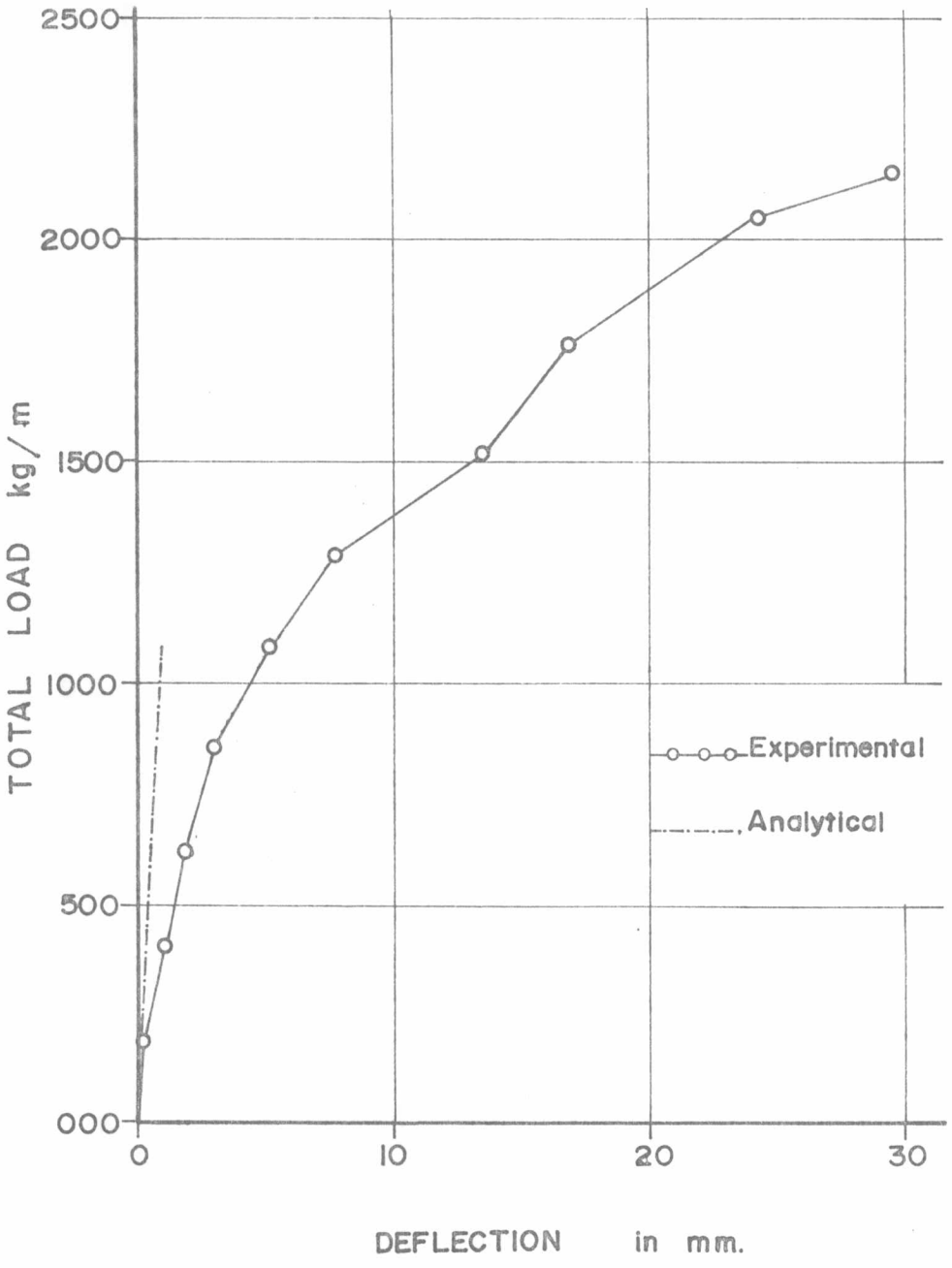

FIGURE 8.7 Z-beam Model; Relation between Load and Centre-span Deflection